Internal Report IASF-BO 594/2011

Analytical approximations for the free free emission amplification factor due to density contrast

T. Trombetti[1,2] and C. Burigana[1,3]

[1] *INAF-IASF Bologna, Via P. Gobetti 101, I-40129, Bologna, Italy*
[2] *Dipartimento di Fisica, Università La Sapienza, P.le A. Moro 2, I-00185 Roma, Italy*
[3] *Dipartimento di Fisica, Università degli Studi di Ferrara, Via G. Saragat 1, I-44100 Ferrara, Italy*

Internal Report IASF-BO/594/2011

24/10/2011

Analytical approximations for the free free emission amplification factor due to density contrast

T. Trombetti[1,2] and C. Burigana[1,3]

[1] *INAF-IASF Bologna, Via P. Gobetti 101, I-40129, Bologna, Italy*
[2] *Dipartimento di Fisica, Università La Sapienza, P.le A. Moro 2, I-00185 Roma, Italy*
[3] *Dipartimento di Fisica, Università degli Studi di Ferrara, Via G. Saragat 1, I-44100 Ferrara, Italy*

SUMMARY – The density contrast of the matter in the universe, related to the evolution of the matter power spectrum, can amplify the signal of the free-free process in the plasma. In this report is described a technique able to derive the variance of the matter power spectrum for different cosmologies and with different values of the cut-off parameter k_{max}, the maximum wave number adopted to integrate the power spectrum for the estimate of the variance. We numerically computed at various redshifts the power spectrum, using a modified version of the code CAMB (the cosmological Boltzmann code for computing the angular power spectrum of the anisotropies of the cosmic microwave background) for various cosmological models and parameters, and a large value of k_{max}, and then numerically integrated it up to the desired value of k_{max} to compute the variance as function of redshift. Suitable analytical approximations of the numerical results are found. This results can be easily implemented in any code dedicated to the CMB spectral distortions to properly compute the amplification of the signal of the free-free process in the plasma because of matter density contrast.

1 Introduction

The density contrast of the matter in the universe, related to the evolution of the matter power spectrum, can amplify the signal of the free-free process in the plasma. In this report we describe an analytical approximation able to derive the amplification correction factor of the free-free parameter, or estimates of its value, with a modified version of CAMB[1] [7], the cosmological Boltzmann code for computing the angular power spectrum (APS) of the anisotropies of the cosmic microwave background (CMB).

2 Matter Power Spectrum

The evolution of the density perturbation power spectrum depends on the nature of the dominant particles in the primordial universe, hence baryonic or non baryonic matter (hot, warm or cold), and on the characteristic of the fluctuations themselves, adiabatic or isothermal, curvature or isocurvature. This modulation on the primordial power spectrum is quantified by the *Transfer Function*.
If $\langle\rho\rangle$ is the mean density of the universe and $\rho(\vec{x})$ the density in the position $\vec{x}$ of the volume, we can define the *density contrast* as [8]:

$$\delta(\vec{x}) = \frac{\rho(\vec{x}) - \langle\rho\rangle}{\langle\rho\rangle}, \tag{1}$$

or, expanding it in terms of the Fourier series, as:

$$\delta(\vec{x}) = \sum_{\vec{k}} \delta_{\vec{k}} \exp(i\vec{k}\cdot\vec{x}), \tag{2}$$

where $\vec{k}$ is the wave number, inversely proportional to the linear dimension of the considered volume of universe:

$$\vec{k} = \frac{2\pi}{L}\vec{n}. \tag{3}$$

The density contrast is defined so that its mean value over the entire volume is null, but in general its variance is not null and is given by the relation:

$$\sigma^2 = \frac{1}{2\pi^2}\int_0^\infty P(k)k^2 dk, \tag{4}$$

where $P(k)$, corresponding to δ_k^2 when one passes to continuous wavenumber and Fourier transform, is the power spectrum of the density perturbation.
The variance depends on time due to the evolution of the fluctuations, and determines the amplitude of the inhomogeneities. If we define a dimensionless quantity that represents the variance contribution per unity logarithmic interval in k,

$$\Delta(k) = \frac{1}{2\pi^2}P(k)k^3, \tag{5}$$

[1] `http://camb.info/`

the variance can be written in the form:

$$\sigma^2 = \int_{-\infty}^{\infty} \Delta(k) d\ln k. \tag{6}$$

3 Transfer Function

The primordial power spectrum, because of the evolution of the perturbations during the linear and non linear regime, gave rise, on large scale, to the structure we observe today, galaxies and clusters of galaxies. If we define the cosmological horizon as the radius $r_H(t)$ of a hypothetical sphere centered on a virtual observer, we can say that a particle is in causal connection with the observer if they are at a distance from each other less or equal to $r_H(t)$, expressed by the relation [8]:

$$r_H(t) = a(t) \int_0^t \frac{cdt'}{a(t')} = \frac{c}{H_0} \frac{a(t)}{a_0} \int_0^{a(t)} \frac{da'}{a'[\Omega_w (a_0/a')^{1+3w} + (1-\Omega_w)]^{1/2}}. \tag{7}$$

When a certain scale with a characteristic perturbation relative to the various components enters the horizon, the spectrum of power at that scale starts to be modulated by different processes operating during the evolution of the universe.
The transfer function $T(k)$ is a quantitative relation that represents the modulation of the primordial power spectrum and is defined as follows:

$$P(k; t_f) = \frac{b^2(t_f)}{b^2(t_p)} T^2(k; t_f) P(k; t_p), \tag{8}$$

where t_p and t_f are respectively an appropriate primordial time, usually the time after the reheating that ends the epoch of inflation, and final time after the modulation epoch, $P(k;t)$ is the power spectrum and $b(t)$ is the linear growth of the perturbation on large scales.

4 Bremsstrahlung process

During the interaction between radiation and ionized matter, the equilibrium distribution function is described by the Planck law, in which the evolution of the photon occupation number is represented by the generalized kinetic equation [4]:

$$\frac{\partial \eta}{\partial t} = \left(\frac{\partial \eta}{\partial t}\right)_C + \left(\frac{\partial \eta}{\partial t}\right)_B + \left(\frac{\partial \eta}{\partial t}\right)_{DC} + \left(\frac{\partial \eta}{\partial t}\right)_{cyc} + \left(\frac{\partial \eta}{\partial t}\right)_{sources}, \tag{9}$$

where the first term in the right hand side is the collision term, hence the Compton scattering (C), and the other terms refer to photon sources, Bremsstrahlung (B), double or Radiative Compton (DC), cyclotron process (cyc) [13] and other possible photon production processes.

The photon distribution law depends on time and on a dimensionless frequency $x = \frac{h\nu}{kT_0}$, where T_0 is the radiation temperature today.

The Kompaneets equation, a suitable approximation of the more general kinetic equation, describes the evolution of the photon occupation number [3]. Considering Compton scattering, Bremsstrahlung and double Compton, it can be expressed by:

$$\frac{\partial \eta}{\partial t} = \frac{1}{t_C x^2 \phi} \frac{\partial}{\partial x} \left[x^4 \left[\phi \frac{\partial \eta}{\partial x} + \eta(1+\eta) \right] \right] + \left[K_B \frac{g_B}{x_e^3} e^{-x_e} + K_{DC} \frac{g_{DC}}{x_e^3} \right] \left[1 - \eta(e^{x_e} - 1) \right], \quad (10)$$

where g_B and g_{DC} are the Gaunt factors and:

$$\begin{cases} x_e = \frac{h\nu}{kT_e} = \frac{x}{\phi} \\ \\ \phi = T_e/T_r \end{cases}, \quad (11)$$

being T_e and $T_r = T_0(1+z)$ the electron and radiation temperature, respectively. The coefficients $K = K(z)$ are given by:

$$\begin{cases} K_B(z) = \frac{8\pi}{3} \frac{e^6 h^2 n_e (n_H + 4n_{He})}{m(6\pi m k T_e)^{1/2} (kT_e)^3} = K_{0B}(z) \phi^{-7/2} \\ \\ \qquad\qquad \text{where} \quad K_{0B} \simeq 2.6 \times 10^{-25} \left(\frac{T_0}{2.7K} \right)^{-7/2} (1+z)^{5/2} \hat{\Omega}_b^2 \quad \sec^{-1} \\ \\ K_{DC}(z) = \frac{4\alpha}{3\pi t_{\gamma e}} \left(\frac{kT_e}{mc^2} \right)^2 \int_0^\infty (1+\eta) \eta x_e^4 dx_e \simeq 8.15 \times 10^{-40} \left(\frac{T_0}{2.7K} \right)^2 \end{cases}, \quad (12)$$

where α is the fine structure constant, $t_{\gamma e}$ the photon electron collision time and t_C the kinetic equilibrium timescale between matter and radiation:

$$\begin{cases} t_{\gamma e} = (n_e \sigma_T c)^{-1} \\ \\ t_C = t_{\gamma e} \frac{mc^2}{kT_e} \simeq 4.5 \times 10^{28} \left(\frac{T_0}{2.7K} \right)^{-1} \phi^{-1} \hat{\Omega}_b^{-1} (1+z)^{-4} \quad \sec \end{cases}. \quad (13)$$

Here, the term $\hat{\Omega}_b$, related to the baryon density in units of the critical density, is defined as:

$$\hat{\Omega}_b = \Omega_b \left[\frac{H_0}{50 \mathrm{Kms}^{-1} \mathrm{Mpc}^{-1}} \right]^2. \quad (14)$$

Eq. 12 makes evident the proportionality of the bremsstrahlung term to the square of the baryon density.

In this work we take into account the density contrast in the intergalactic medium, and we look for a lower limit in the value of the free-free parameter, first in the case of the suppression reionization model in the framework of standard ΛCDM models, and then investigating alternative cosmological models. The correction factor to the free-free amplification parameter is a quantity greater than one. Indeed, if we define the density as the contribution of a mean term plus a small perturbation,

$$n = \langle n \rangle + \delta, \tag{15}$$

and we consider that for the mass conservation law $\langle \delta \rangle = 0$, then

$$\langle n^2 \rangle = \langle n \rangle^2 + \langle \delta^2 \rangle, \tag{16}$$

the correction factor can be expressed by:

$$\frac{\langle n^2 \rangle}{\langle n \rangle^2} = 1 + \frac{\langle \delta^2 \rangle}{\langle n \rangle^2} = 1 + \sigma^2 > 1. \tag{17}$$

5 Cold and Warm Dark Matter models

The Cold Dark Matter (CDM) standard cosmological model forecasts the existence of primordial cold and collisionless particles with negligible small velocity dispersion at the epoch of radiation-matter equality and a derived matter power spectrum supporting small scale structure formation. The distribution of velocities of the dark matter suppresses fluctuations below its free streaming scale (the distance over which a particle travels), which increases with the mean dark matter velocities and decreases with its mass. In this framework galaxy formation is a hierarchical process, resulting in the typical *bottom up* scenario, in which small scales collapse first and merge together leading to clusters of galaxies. Denser clumps, the only that subsist the mergers, give rise to satellite galaxies [2].

Semi-analytical large scale simulations have proved that these CDM candidates, such as WIMPs, cause an over-prediction of satellite galaxies with respect to those observed in the Milky Way.

Within this context emerges the idea of Warm Dark Matter (WDM) particles as a possible solution of the small scales CDM and cuspy halo problems, the latter related to the density profile in virialized DM halos. This distribution function is useful to disentangle between different hypothesis on DM, being characterized by cusps in CDM models, and by smoother profile in observational data.

WDM candidates have intrinsic thermal velocities, so exhibit larger velocity dispersions, compared to CDM particles, and present characteristic free streaming scales, which contribute to determine clustering properties, such that small scale structures formation is suppressed.

Typical particles masses are in the range of the keV scale, which is intermediate between cold and hot DM masses, $m_{warm} \sim (1-10)\ keV$ [1], while the other models give $m_{cold} \sim (10-10^2)\ GeV$ and $m_{hot} \sim$ few eV, and possible candidates are sterile neutrinos or gravitinos.

The suppression of fluctuations due do WDM particles on scales smaller than their free-streaming scale, corresponding to a cut-off of the total matter power spectrum on large wave numbers k, slow down the growth of structure ([11]) and can be described by means of the transfer function imposing different values of the cut-off parameter. For a given cosmological model, it is possible to describe how the matter distribution is affected by the free-streaming length with a relative transfer function provided by the ratio between WDM and CDM power spectrum:

$$T(k) = \left[\frac{P(k)_{WDM}}{P(k)_{CDM}}\right]^{1/2}. \tag{18}$$

The matter power spectrum of the two cosmologies differ only at high wave numbers, as shown in Fig. 1, where the linear power spectrum today ($\log_{10}P(k)$ vs $\log_{10}k\,\mathrm{Mpc\,h}$) for various assumption about DM particles [10] is reported. Note the dropping of $P(k)$ at decreasing k for decreasing mass particle. The case of 1 keV sterile neutrinos is also reported.

While the formation of the first generation of stars is affected by the adopted cosmological model, large scale structure distributions have similar behaviors, regardless of the model [5]. For this reason, in the following analysis we looked for an analytical description of the matter power spectrum assuming a ΛCDM model, but introducing a cut-off wave number k_{max} in the range $[20, 1175]$ that approximately mimics the drops in the power for WDM models with different particle properties.

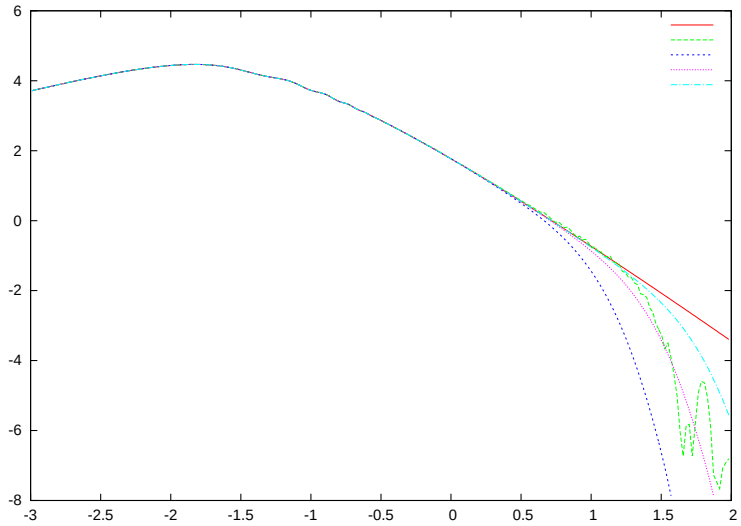

Figure 1: $\log_{10} P(k)$ vs. $\log_{10} k(Mpc)$ for CDM (solid red line) and WDM particles with masses 1 keV (blue dashed line), 2 keV (magenta short dashed line), 4 keV (light blue dot-dashed line) decoupling in equilibrium, and 1 keV sterile neutrinos (green long dashed line). WDM cuts $P(k)$ on small scales. Plot adapted from [10].

6 Suppression model: analytical variance function with a varying k_{max}

Free-free emission from the ionized medium, with the interplay of cosmic radiative feedback of the sources whom reionized the universe, can produce distortions in the CMB primordial spectrum.
In [9] the effect of this process was explored for two different reionization histories, the filtering and the suppression model, under the assumption of a diffuse, averaged density.
In order to derive the variance of the matter power spectrum we run CAMB, the code for the anisotropies in the CMB, setting up the cosmological parameters of the suppression model (see [9]). With reference to the CAMB notation, the cosmological parameters for the suppression model are:

$$\begin{array}{lll} \tau = 0.1017 & n_s = 0.95 & \sigma_8 = 0.74 \\ \Omega_b = 0.0413 & \frac{dn_s}{d\ln k} = 0 & Amp = 2.018 \times 10^{-9} \\ \Omega_{cdm} = 0.1987 & r = 0.1 & z_{reion} = 10 \\ \Omega_\Lambda = 0.76 & h = 73 & w = -1 \end{array} \tag{19}$$

With the CAMB code it is possible to save a file of the evaluated conventionally normalized matter power spectrum for baryons, cold dark matter particles and massive neutrinos in h/Mpc units, and the transfer function in the synchronous gauge, given a unit primordial curvature perturbation on superhorizon scales, for each requested redshift and the parameter that represents the cut-off in the estimate of the variance, i.e. the variable $transfer\_kmax$ of the code. We selected a redshift interval between 0 and 30 with an increasing step of 0.1, and an initial $transfer\_kmax = 1000$ (here after k_{max}).
For the computation of the variance, hence the integration of the power spectrum $P(k)$ as expressed in Eq. 6, we used the routine $D01GAF$ of the NAG libraries that evaluates the integral of a function which is specified numerically at four or more points, over the specified range, using third order finite difference formulae with error estimates, according to a method by Gill and Miller [6].
For this purpose we implemented a Fortran routine which derives the variance for each redshift bin and stores it in a file. At each run we adopted different values for the upper limit of the integration, which correspond to use different values of the input parameter k_{max}, with the NAG routine, such as 20, 50, 100, 150, 200, 250, 300, 350, 400, 500, 600, 700, 800, 850, 900, 1000, to explore the differences in the shape of the curves. What we were looking for was an analytical relation for the whole set of parameters. With this aim we adopted the case $k_{max} = 100$ as a reference. We found for it an analytical relation with the fitting functions of the program *Igor Pro* [12] and searched for a general function able to reproduce the other curves of variance just depending on the variation of the cut-off parameter.
In all cases, the ratio between the variance's reference case and the one at a generic cut-off was best fitted quite well by a linear function of the redshift, for which the intercept and the slope, say $a(k)$ and $b(k)$, depends only on the chosen k_{max}, as shown in Fig. 2

To generalize also this behaviour, we tried to find an universal law for these parameters, able to reproduce the results for any other cut-off's value. We fitted these two new parametric quantities, $a(k)$ and $b(k)$, with the same program as before, and we found an extremely good representation in terms of the function Double Exponential X Offset:

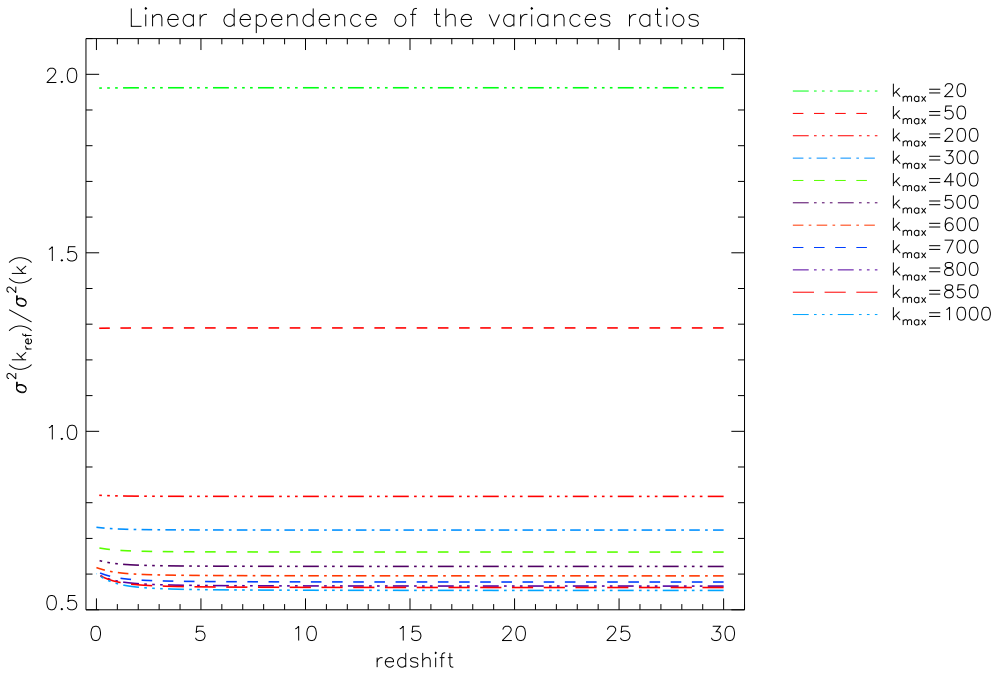

Figure 2: Linear dependence of the ratio between the variance at a generic cut-off and the variance of the reference curve with $k_{ref} = 100$.

$$\begin{cases} fit\_a(k) = a_0 + a_1 \exp(\frac{a_2 - k}{a_3}) + a_4 \exp(\frac{a_2 - k}{a_5}) \\ \\ fit\_b(k) = b_0 + b_1 \exp(\frac{b_2 - k}{b_3}) + b_4 \exp(\frac{b_2 - k}{b_5}) \end{cases}, \tag{20}$$

where the above constants are

$$\begin{cases} a_0 = 0.51385 \\ a_1 = 0.85505 \\ a_2 = 20.0 \\ a_3 = 26.377 \\ a_4 = 0.59601 \\ a_5 = 235.98 \end{cases} \quad \begin{cases} b_0 = -8.9452 \times 10^{-5} \\ b_1 = 4.7704 \times 10^{-5} \\ b_2 = 20.0 \\ b_3 = 0.27323 \\ b_4 = 9.8741 \times 10^{-5} \\ b_5 = 1034.8 \end{cases}, \tag{21}$$

so that we could establish the relation:

$$fit\_line = fit\_a(k) + fit\_b(k)\sigma^2(k). \tag{22}$$

The same functional form was used to fit the variance for the case $k_{max} = 100$, but here we first divided the redshift interval in two subintervals, $z_l \in [0; 9]$ and $z_h \in [9; 30]$:

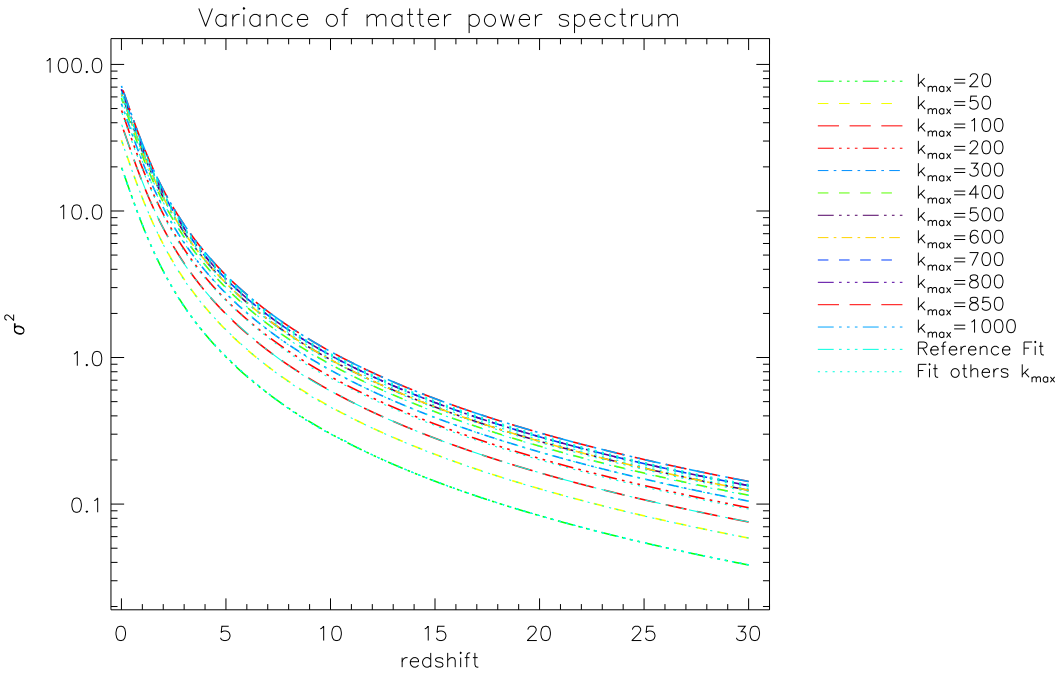

Figure 3: Variance for different values of the cut-off parameter k_{max} with the relative fitting functions. The curve *Reference Fit* is the fit to the $k_{max} = 100$ curve, while *Fit other* k_{max} are the other curves obtained with analytical functions derived from the reference one as explained in the text.

$$\begin{cases} fit\_k_{ref}^{low} = l_0 + l_1 \exp(\frac{l_2 - z_l}{l_3}) + l_4 \exp(\frac{l_2 - z_l}{l_5}) \\ \\ fit\_k_{ref}^{high} = h_0 + h_1 \exp(\frac{h_2 - z_h}{h_3}) + h_4 \exp(\frac{h_2 - z_h}{h_5}) \end{cases} , \tag{23}$$

with:

$$\begin{cases} l_0 = 0.27464 \\ l_1 = 28.58 \\ l_2 = -1.574 \times 10^{-13} \\ l_3 = 0.84439 \\ l_4 = 8.4836 \\ l_5 = 2.9378 \end{cases} \quad \begin{cases} h_0 = 0.033389 \\ h_1 = 0.24724 \\ h_2 = 9.0 \\ h_3 = 2.7819 \\ h_4 = 0.40036 \\ h_5 = 8.9756 \end{cases} \tag{24}$$

From the concatenation of $fit\_k_{ref}^{low}$ and $fit\_k_{ref}^{high}$ we define fit_k_{ref}. Once derived all the fundamental quantities, we could determine the fitting relations for all the variances curves we included in the analysis:

$$\sigma^2_{Fit}(k) = \frac{fit\_k_{ref}}{fit\_line} . \tag{25}$$

The graph of Fig. 3 show the result, and it s possible to see that the analytical variance function, the dotted curve (*Fit others* k_{max}), is reproduced almost exactly compared to the one derived with CAMB code. So the analytical representation is in good approximation with the simulation almost in all cases, as displayed in Fig. 4, where are plotted the relative errors of the variances, with an error at most of 4% except for the two highest cut-off values. This trend is due to the fact that higher values of k_{max} correspond to the more distant curves in respect to the reference one.

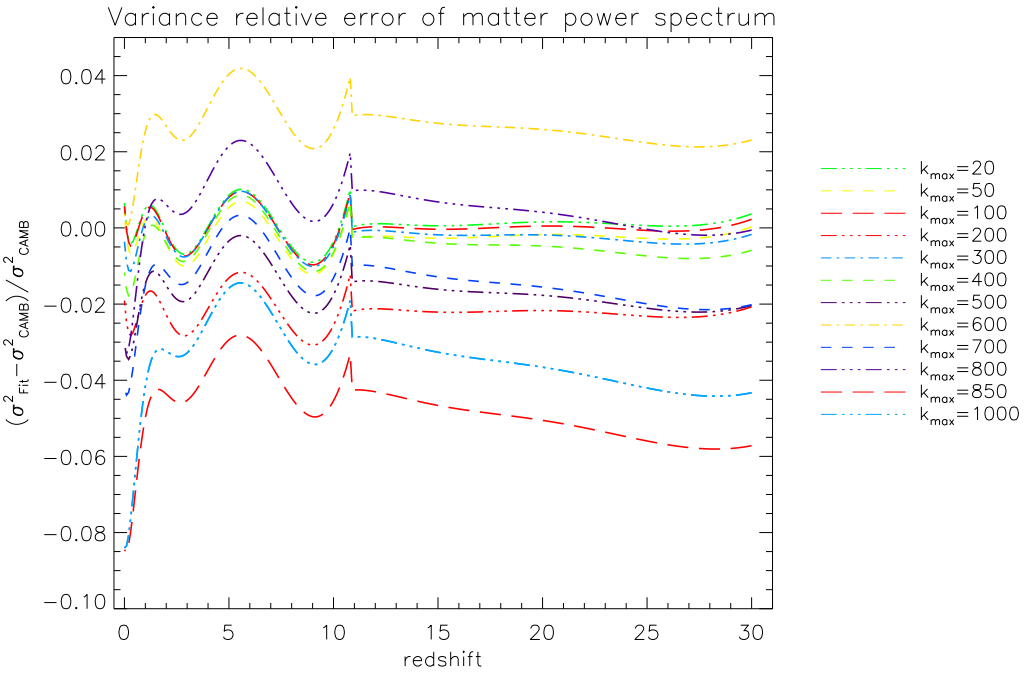

Figure 4: Variance relative errors for the fitting functions of the previous plot.

7 Other cosmological models with a constant cut-off parameter

In this section are shown the results obtained when the same analytical technique is applied to derive the variance given by different cosmologies for a constant value of k_{max}.
For this aim we run the original version of CAMB, assuming a different set of cosmological parameters taken from the *WMAP Seven Year Cosmological Parameters* results[2].

In particular we studied the following theoretical models:

1) Λ-CDM + Run + Tens, the Standard Cosmological model with SZ effect, dark energy, tensors, lensing and running, that parametrizes the variation of the scalar spectral index with respect to the wave number k.

2) W-CDM, in which the dark energy equation of state is allowed vary, hence $w \neq -1$.

[2]See `http://lambda.gsfc.nasa.gov/product/map/dr4/parameters.cfm` for details.

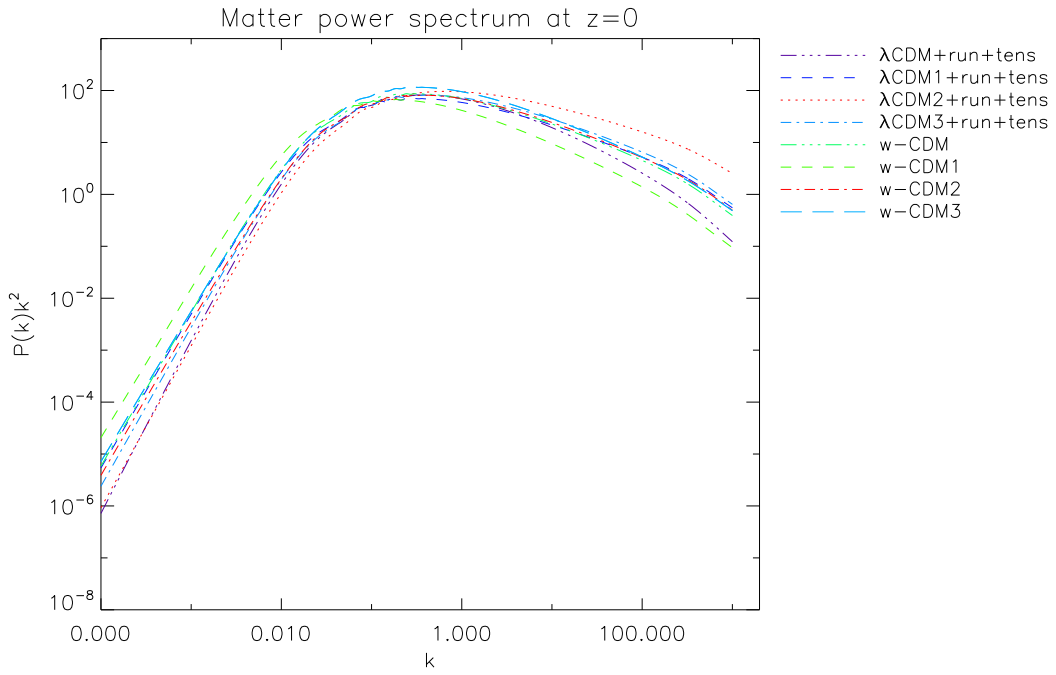

Figure 5: Matter power spectrum at $z = 0$ for the two different cosmologies and their alternative set of parameters.

For each cosmology simulations we have four runs, each of them with a characteristic set of parameters, in agreement within two σ with the WMAP results. The cut-off parameter was fixed to $k_{max} = 1000$. The parameters of each model are:

1a) Λ-CDM:

$$\begin{array}{lll} \tau = 0.0872 & n_s = 1.076 & \sigma_8 = 0.804 \\ \Omega_b = 0.046 & \frac{dn_s}{d\ln k} = -0.048 & Amp = 1.885 \times 10^{-9} \\ \Omega_{cdm} = 0.247 & r = 0.1 & z_{reion} = 11.4 \\ \Omega_\Lambda = 0.707 & h = 69.1 & w = -1 \end{array} \tag{26}$$

1b) Λ-CDM1:

$$\begin{array}{lll} \tau = 0.112 & n_s = 1.01 & \sigma_8 = 0.7716 \\ \Omega_b = 0.0427 & \frac{dn_s}{d\ln k} = 0.007 & Amp = 2.117 \times 10^{-9} \\ \Omega_{cdm} = 0.202 & r = 0.01 & z_{reion} = 13.229 \\ \Omega_\Lambda = 0.7553 & h = 71 & w = -1 \end{array} \tag{27}$$

1c) Λ-CDM2:

$$\begin{array}{lll} \tau = 0.104 & n_s = 1.141 & \sigma_8 = 0.7926 \\ \Omega_b = 0.0509 & \frac{dn_s}{d\ln k} = 0.029 & Amp = 1.582 \times 10^{-9} \\ \Omega_{cdm} = 0.292 & r = 0.03 & z_{reion} = 13.094 \\ \Omega_\Lambda = 0.6571 & h = 66 & w = -1 \end{array} \tag{28}$$

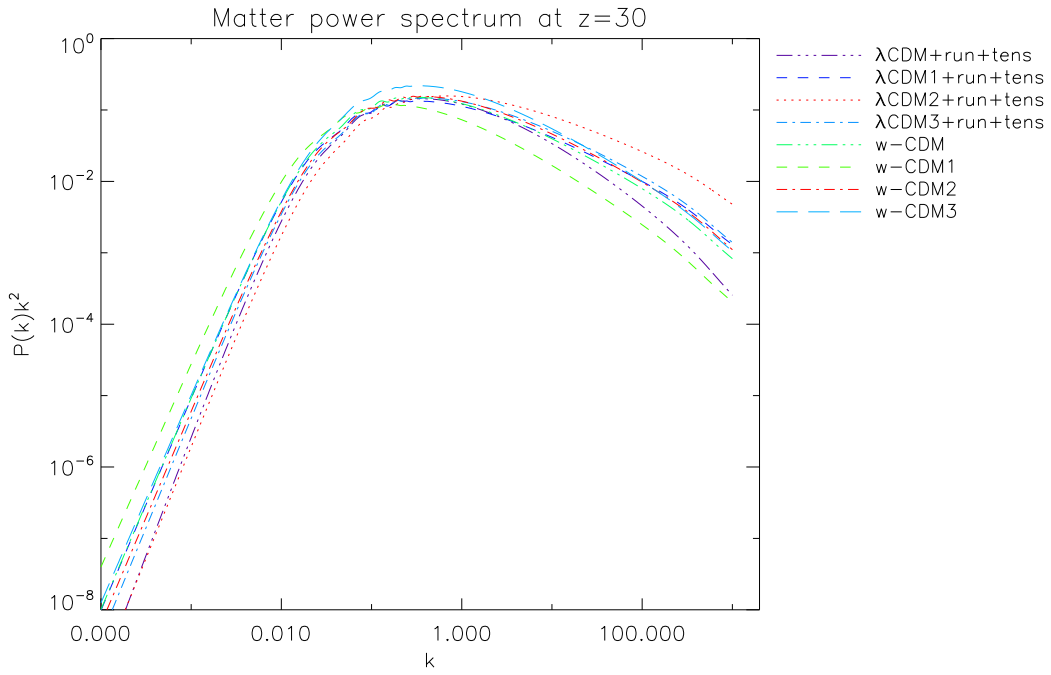

Figure 6: Matter power spectrum at $z = 30$ for the two different cosmologies and their alternative set of parameters.

1d) Λ-CDM3:

$$\begin{array}{lll} \tau = 0.0966 & n_s = 1.05 & \sigma_8 = 0.801 \\ \Omega_b = 0.0487 & \frac{dn_s}{d\ln k} = -0.035 & Amp = 1.852 \times 10^{-9} \\ \Omega_{cdm} = 0.229 & r = 0.07 & z_{reion} = 11.122 \\ \Omega_\Lambda = 0.7223 & h = 73 & w = -1 \end{array} \tag{29}$$

2a) w-CDM:

$$\begin{array}{lll} \tau = 0.088 & n_s = 0.964 & \sigma_8 = 0.857 \\ \Omega_b = 0.044 & \frac{dn_s}{d\ln k} = 0 & Amp = 2.095 \times 10^{-9} \\ \Omega_{cdm} = 0.215 & r = 0.1 & z_{reion} = 10.5 \\ \Omega_\Lambda = 0.741 & h = 75 & w = -1.12 \end{array} \tag{30}$$

2b) w-CDM1:

$$\begin{array}{lll} \tau = 0.104 & n_s = 0.849 & \sigma_8 = 0.798 \\ \Omega_b = 0.022 & \frac{dn_s}{d\ln k} = 0 & Amp = 1.518 \times 10^{-9} \\ \Omega_{cdm} = 0.137 & r = 0.05 & z_{reion} = 14.486 \\ \Omega_\Lambda = 0.841 & h = 90 & w = -1.55 \end{array} \tag{31}$$

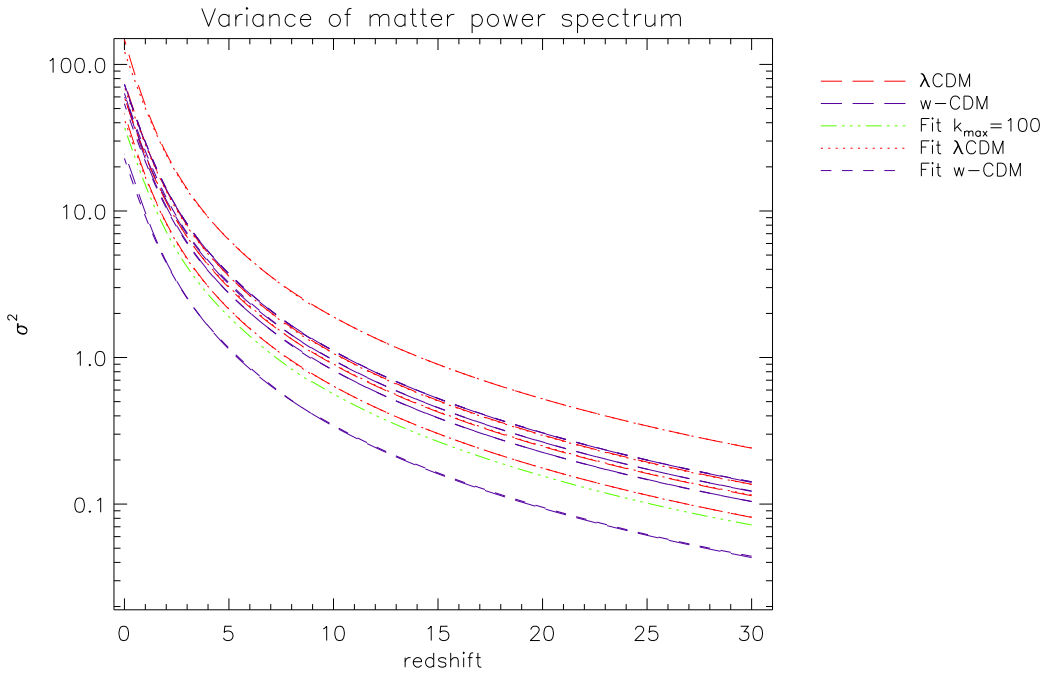

Figure 7: Variance for the two different cosmologies and their alternative set of parameters, which result from the simulations, and with the relative fitting functions derived from the reference curve (see text).

2c) w-CDM2:

$$\begin{array}{lll} \tau = 0.073 & n_s = 0.98 & \sigma_8 = 0.81 \\ \Omega_b = 0.061 & \frac{dn_s}{d\ln k} = 0 & Amp = 2.782 \times 10^{-9} \\ \Omega_{cdm} = 0.297 & r = 0.001 & z_{reion} = 9.742 \\ \Omega_\Lambda = 0.642 & h = 61 & w = -0.72 \end{array} \tag{32}$$

2d) w-CDM3:

$$\begin{array}{lll} \tau = 0.097 & n_s = 0.911 & \sigma_8 = 0.97 \\ \Omega_b = 0.037 & \frac{dn_s}{d\ln k} = 0 & Amp = 2.282 \times 10^{-9} \\ \Omega_{cdm} = 0.252 & r = 0.005 & z_{reion} = 13.138 \\ \Omega_\Lambda = 0.711 & h = 78 & w = -0.88 \end{array} \tag{33}$$

In the whole set of run, even if k_{max} was fixed to 1000, for the derivation of the variance we considered in the numerical integration only the data till $k_{max} = 100$.
In Fig. 5 and 6 are plotted the matter power spectrum at $z = 0$ and $z = 30$, respectively, for the considered models.
In both cases the trend is very similar; differences between models are more evident at small scales and tend to be smaller on intermediate scales.

From the plots at different redshift it is evident the variation of the shape of the variance, particularly on small scales, which is related to the entire set of cosmological parameters and not only to the amplitude.

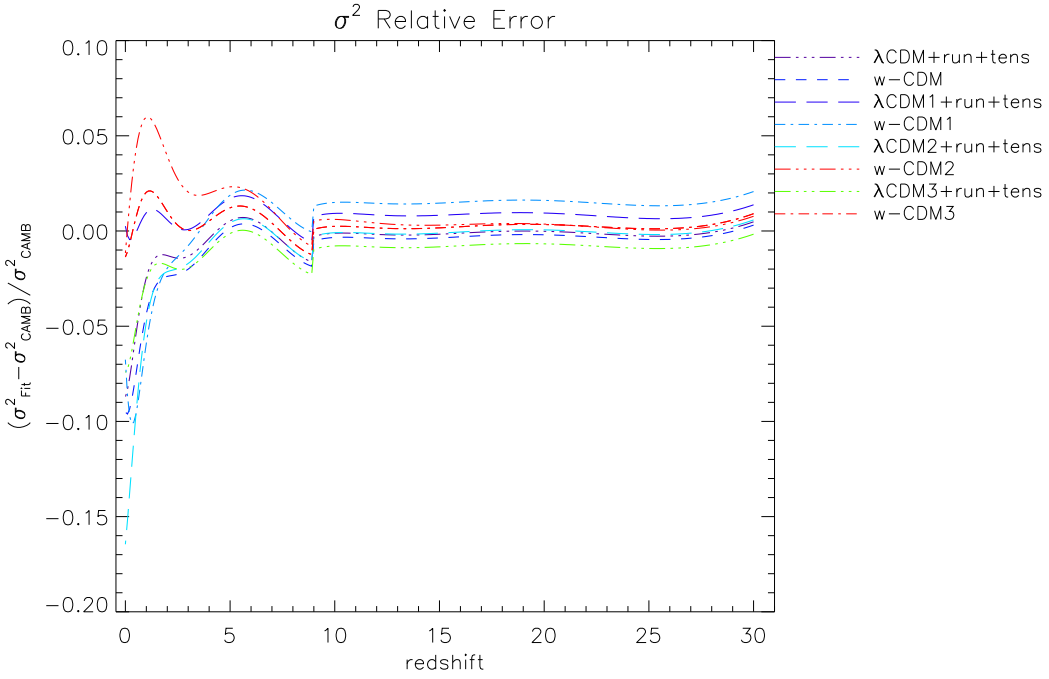

Figure 8: Relative error of the variance for the models analyzed.

We assumed that, for the determination of the σ^2, we could take into account the same reference curve at $k_{max} = 100$ we adopted in the case of the suppression model (so in the modified version of CAMB). The main difference with the previous analysis is that now we are always studying the limiting case $k_{max} = 100$. In this context, for this reason, the coefficients $a(k)$ and $b(k)$ are constants and independent on k.

To reproduce the right shape of the variance for each model, we must multiply the reference curve for a correction factor which depends on the specific model, and so here is not possible to find out a general law. This multiplicative factor let us to shift the curves, along the y axis, to fit the ones derived with CAMB, and is given below for the various models:

1) Λ-CDM: $corr\_fact = 1.131$

2) Λ-CDM1: $corr\_fact = 1.603$

3) Λ-CDM2: $corr\_fact = 3.354$

4) Λ-CDM3: $corr\_fact = 1.889$

5) w-CDM: $corr\_fact = 1.447$

6) w-CDM1: $corr\_fact = 0.611$

7) w-CDM2: $corr\_fact = 1.705$

8) w-CDM3: $corr\_fact = 1.968$

To better understand the reason why we need to apply a correction factor to the ratio between the fitted curves and the reference curve at $k_{max} = 100$, we looked for a possible

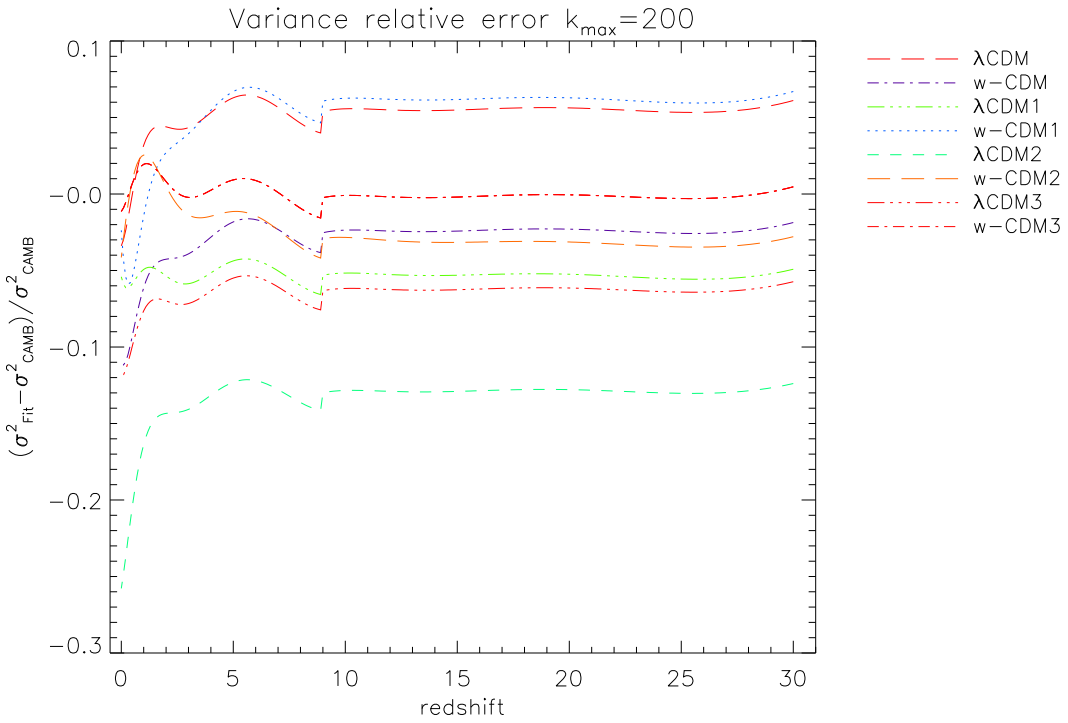

Figure 9: Relative error of the variance.

proportionality of the variance with respect to the amplitude of the power spectrum assumed at each run.

In Fig. 7 we show the variance for the two cosmologies analyzed and for the various set of parameters, hence 4 curves for each model, with the fitting curves derived from the reference one (the green dash dotted line).

In Fig. 8 is shown the relative error of the variance's fitting functions with respect to the variance's functions simulated. The bigger is the error, the lower is the redshift, especially in a redshift range between 0 and ~ 10, a time interval that corresponds to the reionization epoch.

8 Cosmological models with variable cut-off parameter

In this section we illustrate the variance's analytical relations we deduced taking into account the same cosmological models as the previous section, and allowing the parameter k_{max} to vary. The starting point is the reference's fitting curve of the suppression model at $k_{max} = 100$, and the corresponding fitting curves obtained for the diverse models.
We analyzed the cases: $k_{max} = 200$, 400, 600, 800 and 1000.
The relation that approximate the variance of these models depending on the cut-off, with an error at most 20%, except for the $\Lambda - CDM2$ model for which the error is almost 40%, is:

$$\begin{cases} \sigma^2_{mod}(k_{ref}) = \sigma^2_{sup}(k_{ref}) \times corr\_fact \\ \\ \sigma^2_{mod}(k) = \sigma^2_{mod}(k_{ref}) \frac{1}{fit\_line(k)} \end{cases} , \tag{34}$$

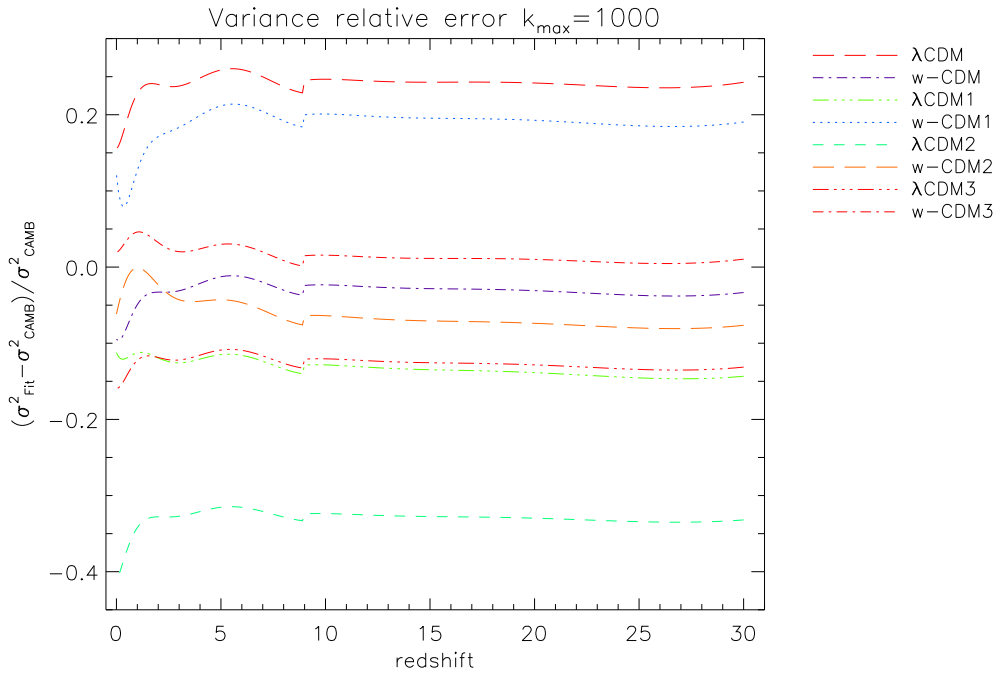

Figure 10: Relative error of the variance.

where $k_{ref} = 100$ is the reference cut-off parameter, $\sigma^2_{mod}(k)$ and $\sigma^2_{sup}(k)$ are, respectively, the variances of the generic and the suppression model and $fit\_line(k)$ is the fitting function of Eq. 25.

In Fig. 11 we report the case of the $k_{max} = 200$. The variance resulting from the models (long dashed lines in red and violet for the two kind of models) and from the fitting functions extrapolated from the approximation explained before (dotted and short dashed lines) are shown. In Fig. 12 we report the same plot but in the extreme case $k_{max} = 1000$, that represents the worst fitting case, due to the fact that the cut-off is the farthest from the reference curve, also noticeable by the comparison of the two graphs.

In Fig. 9 and Fig. 10 the relative errors of the variance for these two limiting cases of the cut-off are shown. As said before, we obtain a more precise result for an assumed cut-off variance near to the reference one.

8.1 Scaling with perturbation amplitude

For what concern the connection between the scaling factor of the matter power spectrum with its relative amplitude and the variance, we investigate a model in which, fixing the cosmological parameters for different simulations, we varied the perturbation amplitude in such a way to achieve at $z = 0$ a σ_8 parameter inside the error given by the model itself. For the test we choose the $\Lambda - CDM$ model, with running and tensors as usual, where a run was set with the same parameters of the case $1a$, $Amp_1 = 1.885 \times 10^{-9}$, while for the other run was set $Amp_2 = 2.011 \times 10^{-9}$ with a resulting $\sigma_8 = 0.831$. From the ratio of the amplitudes of the two simulations we have:

$$\frac{Amp_1}{Amp_2} = 0.93735. \tag{35}$$

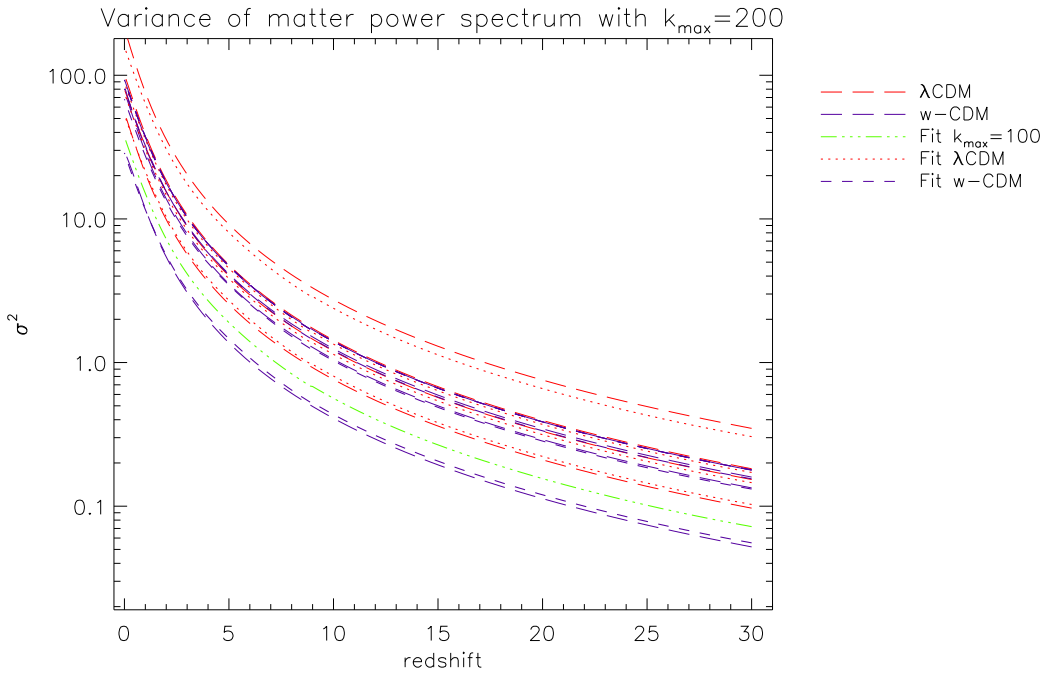

Figure 11: Variance of matter power spectrum and their relative fitting functions.

When integrating the power spectrum for the derivation of the variance, computing the ratio between them (one for each model) and the mean value, we obtain: 0.93742. So, to a very good level of approximation, we can affirm that both of them, the matter power spectrum and the variance, follow a scaling law proportional to the perturbation amplitude and, at the same time, they are characterized by a common shape.

9 Conclusion

In this report is described a technique able to derive the variance of the matter power spectrum for different cosmologies and with different values of the cut-off parameter k_{max}, the maximum wave number adopted to integrate the power spectrum for the estimate of the variance (see Eq. 4). We numerically computed at various redshifts the power spectrum using the code CAMB for various cosmological models and parameters, and a large value of k_{max} and then numerically integrated it up to the desired value of k_{max} to compute the variance as function of redshift. Suitable analytical approximations of the numerical results are found. They allow to reproduce the numerical results at each redshift with an accuracy always better than few per cent assuming the same cosmological model and with an accuracy better than about 10 per cent of 20 per cent when a cosmological model different from the reference one is considered, the larger error referring to larger adopted value of k_{max}. Of course, the method can be generalized starting from any cosmological reference model to improve the accuracy in the desired cases. This results can be easily implemented in any code dedicated to the CMB spectral distortions to properly compute the amplification of the signal of the free-free process in the plasma because of matter density contrast. This work links the output of tools dedicated to anisotropies and inhomogeneities in the universe with tools dedicated to CMB spectral distortions.

Acknowledgements – We acknowledge support by MIUR through PRIN 2009.

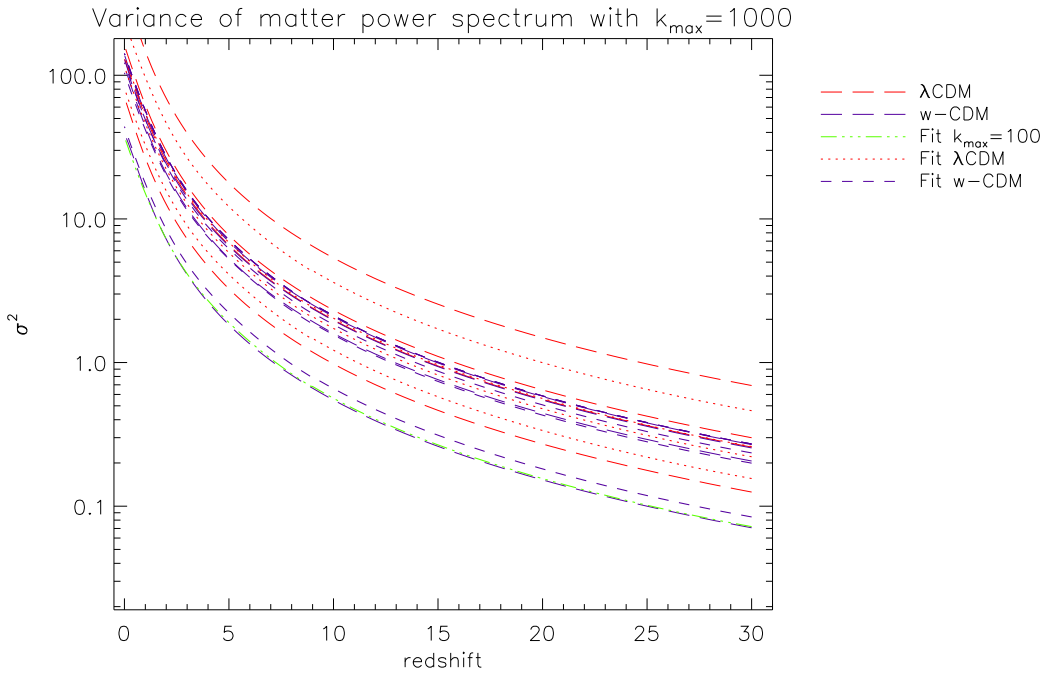

Figure 12: Variance of matter power spectrum and their relative fitting functions.

References

[1] D. Boyanovsky, H.J. de Vega, N.G. Sanchez, 2008, Physical Review D, Vol. 77, Issue 4, id. 043518

[2] D. Boyanovsky and J. Wu, 2011, Small scale aspects of warm dark matter: Power spectra and acoustic oscillations, Physical Review D, Vol. 83, Issue 4, id. 043524

[3] C. Burigana, G. de Zotti, L. Danese, 1995, Analytical description of spectral distortions of the cosmic microwave background, Astronomy and Astrophysics, Vol. 303, p. 323-330

[4] L. Danese and G. De Zotti, 1977, The relic radiation spectrum and the thermal history of the Universe, Nuovo Cimento, Rivista, Serie 2, Vol. 7, p. 277-362

[5] L. Gao and T. Theuns, 2007, Lighting the Universe with Filaments, Science, Vol. 317, Issue 5844, p. 1527-1530

[6] P.E. Gill and G.F. Miller, 1972, An algorithm for the integration of unequally spaced data, Comput. J., Vol. 15, p. 80-83

[7] A. Lewis, A. Challinor, A. Lasenby, 2000, Efficient Computation of CMB anisotropies in closed FRW models, ApJ, Vol. 538, p. 473-476

[8] F. Lucchin, 1998, Introduzione alla cosmologia, Zanichelli ed.

[9] R. Salvaterra, C. Burigana, R. Schneider, T.R. Choudhury, A. Ferrara, L.A. Popa, 2009, Cosmic radiative feedback from reionization, Mem. S.A.It., Vol. 80, p. 26-29

[10] N.G. Sanchez, 2011, in http://chalonge.obspm.fr/colloque2011.html

[11] M. Viel, J. Lesgourgues, M.G. Haehnelt, S. Matarrese, A. Riotto, 2005, Constraining warm dark matter candidates including sterile neutrinos and light gravitinos with WMAP and the Lyman-α forest, Physical Review D, Vol. 71, Issue 6, id. 063534

[12] WaveMetrics Inc. 2010, Igor Pro (version 6.2)

[13] A. Zizzo and C. Burigana, 2005, On the effect of cyclotron emission on the spectral distortions of the cosmic microwave background, New Astronomy, Vol. 11, Issue 1, p. 1-16